Random lasing mode alterations by single-nanoparticle perturbations

Seung Ho Choi and Young L. Kim[a)]
Weldon School of Biomedical Engineering, Purdue University, West Lafayette, Indiana 47907, USA

(Received 26 August 2011; accepted 9 November 2011; published online 23 January 2012)

We numerically demonstrate that alterations in random lasing modes can serve as a highly sensitive biosensing mechanism for single-nanoparticle quantitation. In our approach, subtle perturbations from a single nanoparticle can induce dramatic changes in multiple eigenmodes in disordered structures that can be detected by spectral variations of lasing emission peaks. Several resonance mode frequencies show relatively linear spectral responses to nanoscale perturbations, and each mode possess different levels of perturbation sensitivity. We also show that such behavior exists in both highly and loosely packed disordered media. We envision that the simplicity of such realization will facilitate the biosensor development using random lasers. © *2012 American Institute of Physics*. [doi:10.1063/1.3675885]

Advances in biosensors and bioassays heavily rely on applications of enabling physical concepts and phenomena. We have recently demonstrated an alternative physical concept for highly sensitive biosensors, by exploiting an intriguing light confinement phenomenon as known as random lasing.[1] In random lasing, resonant cavities are self-generated by a group of individual scatterers in a disordered structure, leading to laser amplification (i.e., amplified spontaneous emission (ASE) random lasers) or laser oscillation (i.e., coherent random lasers). ASE random lasers showed sensing applications for temperature sensing[2] and explosive detection.[3] In particular, we have shown that coherent random lasers can be used to detect a small number of nanoparticles and extremely small strains.[1] Because coherent random lasers possess multiple discrete peaks and their frequency positions are highly reproducible in fixed or static structures,[4] they can be excellent candidates for biosensing mechanisms. However, the feasibility that coherent random lasing can be used to assess minute optical perturbations even in a single nanoparticle has not yet been tested. Single-nanoparticle quantitation is critical for single-virus, single-bacterium, and single-biomolecule detections. In this letter, our numerical experiments reveal the following characteristics: (1) Random lasing modes can provide a means to amplify perturbations at single-nanoparticle levels. (2) Such perturbations can induce changes in multiple resonance modes, some of which possess linear spectral responses with different sensitivities. (3) Such characteristics can exist in both highly and loosely packed disordered structures.

We numerically investigate 2-dimensional (2-D) resonant modes by considering E_z, H_x, and H_y components of the TM mode, in which the electrical field is along the cylinder axis, in a similar fashion to our previous studies.[1] We calculate the complex eigenvalue of eigenmode κ ($= \mathrm{Re}(\kappa) + \mathrm{i}{*}\mathrm{Im}(\kappa)$, where the real and imaginary parts represent resonant frequencies and losses, respectively) of the passive system (i.e., quasimodes). We use a finite element method (FEM) to solve the Helmholtz equation that can directly access individual quasimodes of the passive system consisting of a large number of nanoparticles ($<$ the wavelength λ). Because random lasing modes are eigenstates of the system, any eigenstate can be a candidate of the lasing modes in coherent random lasers. The FEM formulated Helmholtz equation has the form of the generalized eigenvalue problem, and the solution (i.e., eigenvalue and eigenmode) can be computed using an unsymmetric multifrontal sparse lower and upper triangular matrices (LU) factorization method (UMFPACK linear system solver). For boundary conditions, we apply a perfectly matched layer to the surrounding medium of the scatterers. In a strongly scattering regime, quasimodes are shown to be identical to actual lasing modes with a gain, which can be calculated using the Maxwell's equations with the rate equation.[5] Although in a weakly scattering regime, lasing modes (i.e., actual lasing modes in the active medium) could be different from the quasimodes,[5] they are still associated with individual quasimodes of the passive system. Indeed, it was shown that the

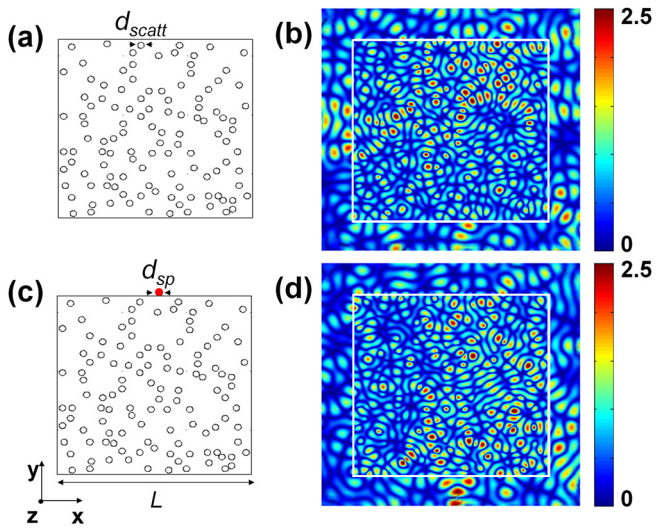

FIG. 1. (Color online) (a) and (c) Simulated structures before and after the single nanoparticle (i.e., red solid circle) is introduced on top of the structure, respectively. (b) and (d) Electric field amplitudes from a representative eigenmode (i.e., mode group # 4 in Figure 2) before and after the single-nanoparticle perturbation, respectively. The white square inside the field delineates the square of the boundary.

[a)]Author to whom correspondence should be addressed. Electronic mail: youngkim@purdue.edu.

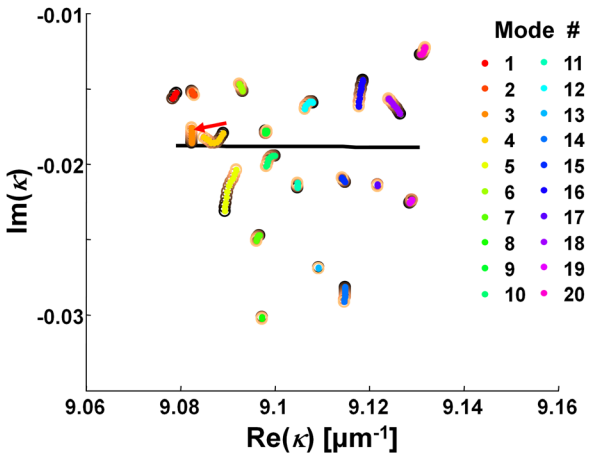

FIG. 2. (Color online) (a) Complex frequencies of the passive system in the scattering medium of $\Phi = 10\%$ and $N = 115$ upon the single-nanoparticle perturbations.

first lasing mode in a uniform gain medium can correspond to its quasimode.[6] Thus, our quasimode study is valid to test our hypothesis.

As shown in Figures 1(a) and 1(c), our first structure consists of randomly distributed nanoparticles of diameter d_{scatt} with the refractive index n_{scatt}, and the surface filling fraction Φ embedded in the square of $L^2 = 6\,\mu\text{m} \times 6\,\mu\text{m}$. The medium outside the square is air $n_0 = 1$. Our numerical experiments can be considered to be nanoparticles embedded in a polymer: SU-8 for the filling medium $n = 1.58$ and TiO_2 for the scatterers with $n_{scatt} = 2.49$ and $d_{scatt} = 200\,\text{nm}$. The values of d_{scatt}, n_{scatt}, Φ, and L are further chosen to achieve two representative configurations. In the case of $\Phi = 10\%$ (the number of nanoparticles $N = 115$), because the effect of interparticle correlation is relatively minimal ($n_{scatt}d_{scatt}/\lambda \leq 0.8$), the independent scattering theory using Mie calculations can be used to estimate a corresponding transport mean free path $l_s \sim 4\,\mu\text{m}$. When $\Phi = 1\%$ ($N = 11$), $l_s \sim 117\,\mu\text{m}$. To imply various single-biomolecule, single-bacterium, and single-virus quantitations, a single nanoparticle ($d_{sp} = 200\,\text{nm}$) is positioned in the middle of the top of the structure and its refractive index gradually increases from $n_{sp} = 1$ to 1.462. In our simulation, we choose that the binding site is localized only in the middle of the top as shown in Figure 1(c). To avoid any numerical errors originating from the mesh regeneration, the mesh size is significantly smaller than the wavelength and n_{sp} is continuously varied without changing the geometries and the corresponding meshes of the structure.

In Figures 1(b) and 1(d), we first show the overall physical concept for the detection of subtle nanoscale alterations at single-nanoparticle levels, taking advantage of mode alterations in the photonic structure. Upon introducing the nanoparticle (red solid circle in Figure 1(d)) on top of the structure, the spatial distribution of the electric field amplitude is significantly altered. This change in the field distribution at a representative mode (i.e., mode group # 4 in Figure 2) strongly indicates that our approach using mode alterations for single-nanoparticle detection is feasible. Indeed, random lasing in a disordered medium is an open system with a strong coupling to the environment as a partially or fully disordered structure.

In Figure 2, we describe numerical results in the scattering medium of $\Phi = 10\%$ and $N = 115$. Figure 2 shows all of the quasimodes in the range of $\text{Re}(\kappa) = 9.07$–9.14 [μm^{-1}] (central $\lambda \sim 690\,\text{nm}$). We depict changes in the quasimodes as n_{sp} is continuously varied from 1 to 1.462. $n_{sp} = 1$ corresponds to the absence of the single nanoparticle. The open colored circles represent the complex frequencies of the modes, and the edge color gradually changes from black to orange in the direction of the red arrows. To trace each mode for different n_{sp}, we group them according to their frequency space trajectory using principal component analysis.[7] Then, 20 groups are marked by the corresponding face colors. As a reference value for quality Q factors, we draw an average Q factor (black solid line) of the complex frequency at $n_{sp} = 1$: $Q_{avg} = |\sum^{M}_{m=1} \text{Re}(\kappa)/(M^2 \sum^{M}_{m=1} 2*\text{Im}(\kappa))|$, where m is the mode number and M is the total number of modes. The alterations in the single nanoparticle induce the changes in the multiple modes, which can be detected by a shift in any of the multimodes. Such alterations in multimodes will be experimentally realized in spectral changes in the emission peaks.

In Figure 3, we select four representative mode groups (i.e., mode group # = 4, 13, 16, and 18) that show highly linear spectral responses. We plot changes in the wavelength shift (Figure 3(a)) as a function of n_{sp} of the single nanoparticle. The linear correlation coefficients, which measure the strength of linear association between the wavelength shift and n_{sp}, are 0.9871, 0.9947, 0.9939, and 0.9998 for the mode group # = 4, 13, 16, and 18, respectively. To further quantify the sensitivity of each mode frequency, we define the sensitivity as the ratio of the wavelength λ_m shift to n_{sp} such that the sensitivity of the m-th quasimode S_m can be expressed

$$S_m = \frac{d\lambda_m}{dn_{sp}}. \tag{1}$$

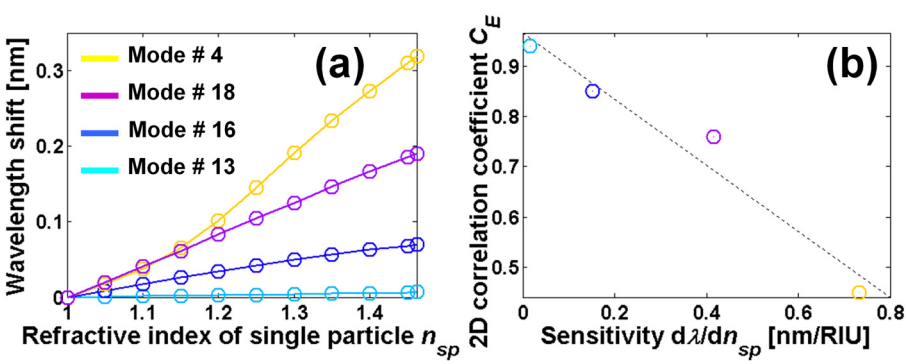

FIG. 3. (Color online) (a) Wavelength shifts of the four selected quasimodes as a function of refractive index n_{sp} of the single nanoparticle. (b) Relationship between the sensitivity of each mode frequency S_m and 2-D correlation coefficients C_E of the electric field difference $\Delta|E|$ between before and after the single-nanoparticle introduction.

As shown in Figure 3(a), each mode has different sensitivity and the each sensitivity can be calculated by linearly fitting the data, because in the selected modes the derivative of the spectral shift over n_{sp} is relatively constant. To better understand the different sensitivity for each mode frequency, we calculate 2-D correlation coefficients C_E of the spatial distribution of the field amplitude difference $\Delta|E|$ between before $|E^{before}(x,y)|$ (when $n_{sp}=1$) and after $|E^{after}(x,y)|$ (when $n_{sp}=1.462$) the perturbations (Figure 4) such that $C_E=\sum_x\sum_y\left(|E^{before}|-\overline{|E^{before}|}\right)\left(|E^{after}|-\overline{|E^{after}|}\right)/\sqrt{\left(\sum_x\sum_y\left(|E^{before}|-\overline{|E^{before}|}\right)\right)\left(\sum_x\sum_y\left(|E^{after}|-\overline{|E^{after}|}\right)\right)}$. Figure 3(b) shows that S_m is inversely correlated to C_E and the linear correlation coefficient between C_E and S_m is -0.96. Overall, the results show that the mode alterations can be accurately captured by linear wavelength shifts, given that the perturbations are extremely small. We further confirm that the linear spectral behavior breaks when the system undergoes a significant change in the overall structure, for example, when we change n_{scatt} of all of the 115 nanoparticles from 1.58 to 1.68 with a step of 0.02 (data are not shown). In such a case, changes in the modes are completely unpredictable and the modes cannot be grouped any more according to their trajectories in the frequency space.

In details, Figure 4 visualizes normalized field alterations upon the single-nanoparticle alterations, because the resonant wavelength is related to the spatial field distribution. The gray scale images represent the field amplitude distribution before introducing the nanoscale perturbations ($n_{sp}=1$). The red and blue scale areas on the gray field images represent the spatial distribution of the field amplitude difference $\Delta|E|$. Figure 4 supports the result shown in Figure 3(b). The amplitude of the electrical field of each mode is significantly altered by the change in n_{sp} of the same single-nanoparticle, with the different sensitivity. In addition to the detection of emission spectra, such spatial distribution of individual lasing modes could potentially be obtained by adjusting the pumping power, placing a narrow bandpass filter in the emission or mapping random lasing cavities.[8]

Figure 5 show similar analyses for the system with $\Phi=0.01$ ($N=11$). We also find relatively linear responses of the wavelength shift in the selected modes, as shown in Figure 5(b). This result supports the idea that loosely packed media could also be adapted as a nanoscale sensing platform.

The benefit of our biosensing approach is the simplicity of realization without high precision nanofabrication. Although there are recent advances in the defect-free periodic photonic structures fabrication, unavoidable variations and imperfections in photonic crystal structures still introduce

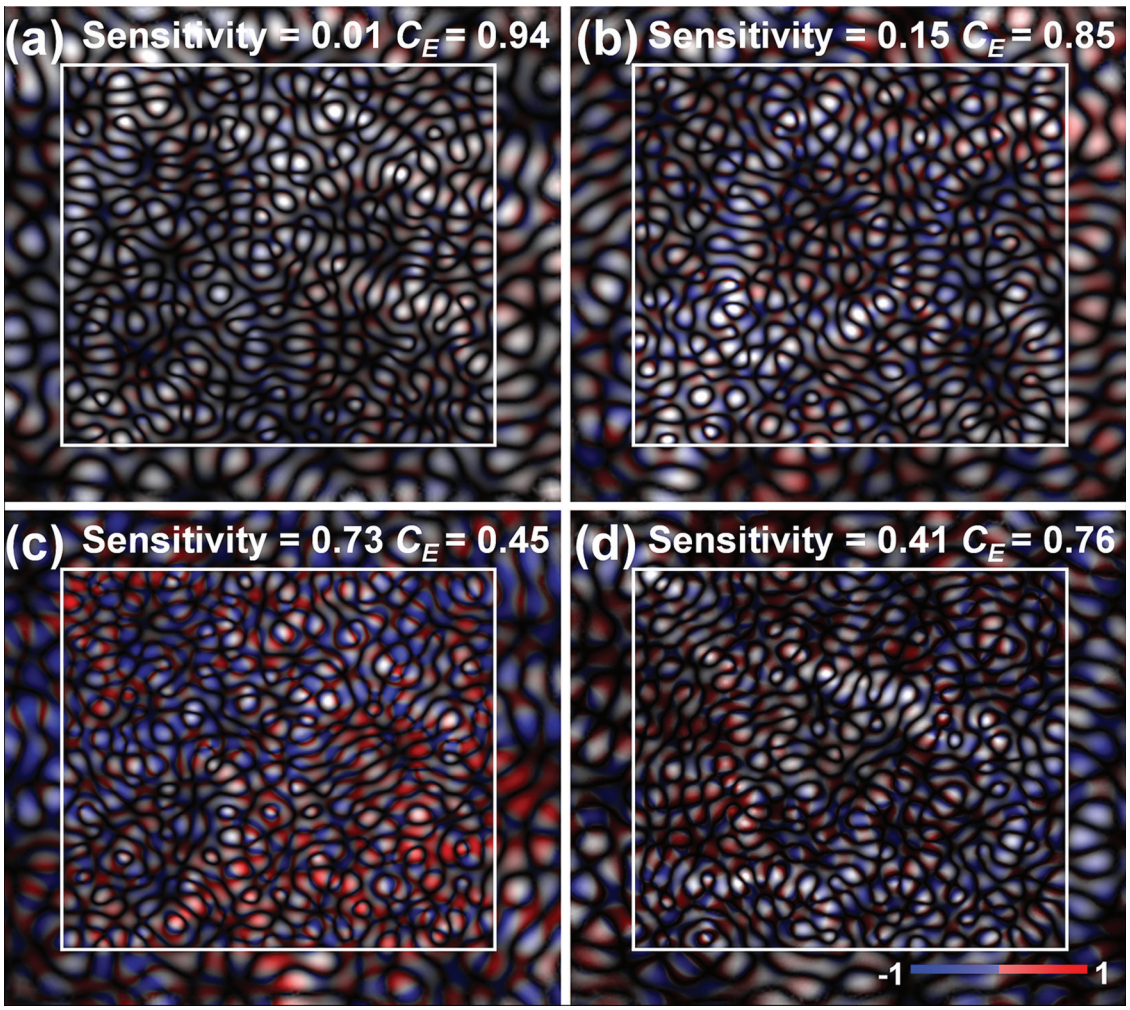

FIG. 4. (Color) (a)–(d) Comparison of the normalized field changes upon the single-nanoparticle perturbations for mode group # = 13, 16, 4, and 18, respectively. To quantify the field difference, 2-D correlation coefficient C_E is calculated.

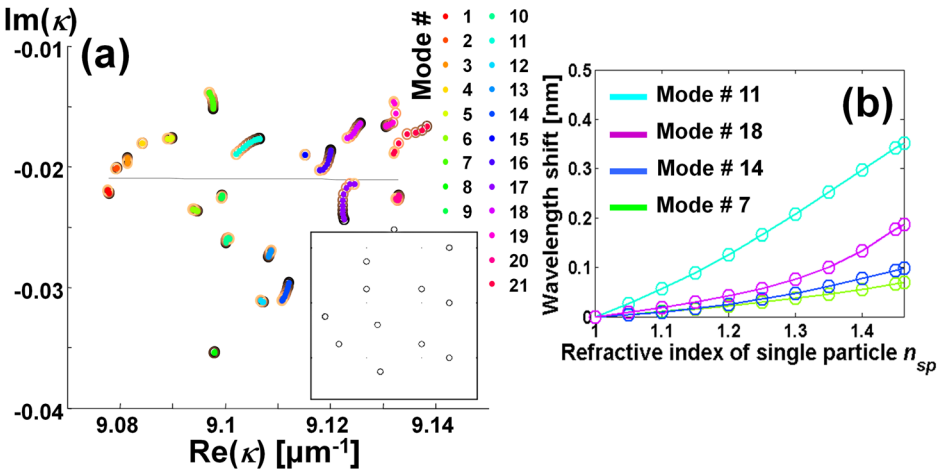

FIG. 5. (Color online) (a) Complex frequencies of the passive system in the scattering medium of $\Phi = 1\%$ and $N = 11$ upon the single-nanoparticle perturbations. (b) Relatively linear spectral responses of the selected quasimodes.

detrimental effects in their performance. A potential limitation in our approach is that the high excitation energy in random lasers could hamper practical and widespread applications. In this respect, several studies were conducted to reduce the lasing threshold using photonic crystal structures,[9] photonic bandgaps (edges of stop bands),[10] 1-D photon localization,[11] and surface plasmon resonance.[12] These methods could potentially be incorporated into our biosensing method.

In conclusion, our studies show the feasibility of the biosensing modality that random lasing modes can provide a means to dramatically amplify subtle nanoscale perturbations at the single-nanoparticle level to readily detectable spectral changes. Nanoscale alterations can induce dramatic changes in the spatial profile of the self-formed optical cavities that can be measured by the spatial distributions or spectral variations of random lasing modes. This characteristic can be advantageous over other conventional biosensing methods that rely on single peaks or single modes. Alterations in resonance modes to nanoscale optical perturbations in disordered media could be accurately captured by linear wavelength shifts of the emission peaks in the spectrum. We note that the low dimensionality (i.e., 2-D structures compared to 3-D structures) in our simulation can enhance light confinement that in turn increases lifetimes of random lasing modes. However, our results indicate that the perturbation sensitivity of mode frequencies could exist in both highly and loosely packed disordered structures. Overall, these unique and intriguing characteristics of coherent random lasers could potentially be transformed into a wide range of sensing platforms (e.g., spectroscopic, multiplexed, or imaging schemes) for biological, chemical, and environmental applications.

We acknowledge the support for S.H. Choi from the Ross Fellowship and Abbott Laboratories.

[1]Q. Song, S. Xiao, Z. Xu, J. Liu, X. Sun, V. Drachev, V. M. Shalaev, O. Akkus, and Y. L. Kim, Opt. Lett. **35**(9), 1425 (2010); Q. Song, S. Xiao, Z. Xu, V. M. Shalaev, and Y. L. Kim, Opt. Lett. **35**(15), 2624 (2010); Q. Song, Z. Xu, S. H. Choi, X. Sun, S. Xiao, O. Akkus, and Y. L. Kim, Biomed. Opt. Express **1**(5), 1401 (2010).
[2]D. S. Wiersma and S. Cavalieri, Nature **414**(6865), 708 (2001).
[3]A. Rose, Z. G. Zhu, C. F. Madigan, T. M. Swager, and V. Bulovic, Nature **434**(7035), 876 (2005).
[4]K. L. van der Molen, R. W. Tjerkstra, A. P. Mosk, and A. Lagendijk, Phys. Rev. Lett. **98**(14), 143901 (2007); S. V. Frolov, Z. V. Vardeny, K. Yoshino, A. Zakhidov, and R. H. Baughman, Phys. Rev. B **59**(8), R5284 (1999); X. H. Wu and H. Cao, Opt. Lett. **32**(21), 3089 (2007).
[5]J. Andreasen, A. A. Asatryan, L. C. Botten, M. A. Byrne, H. Cao, L. Ge, L. Labonté, P. Sebbah, A. D. Stone, H. E. Türeci *et al.*, Adv. Opt. Photon. **3**(1), 88 (2011).
[6]C. Vanneste, P. Sebbah, and H. Cao, Phys. Rev. Lett. **98**, 143902 (2007).
[7]H. Trevor, T. Robert, and F. Jerome, *Hierarchical Clustering: The Elements of Statistical Learning*, 2nd ed. (Springer, New York, 2009).
[8]R. C. Polson and Z. V. Vardeny, Opt. Lett. **35**(16), 2801 (2010).
[9]A. Yamilov and H. Cao, Phys. Rev. A **69**(3), 031803(R) (2004).
[10]V. I. Kopp, B. Fan, H. K. M. Vithana, and A. Z. Genack, Opt. Lett. **23**(21), 1707 (1998).
[11]V. Milner and A. Z. Genack, Phys. Rev. Lett. **94**(7), 07390 (2005).
[12]X. G. Meng, K. Fujita, S. Murai, T. Matoba, and K. Tanaka, Nano Lett. **11**(3), 1374 (2011).